

Under-ice acoustic navigation using real-time model-aided range estimation

EeShan C. Bhatt,^{1,2, [a](#)} Oscar Viquez,² and Henrik Schmidt^{2, [b](#)}

¹*MIT-WHOI Joint Program in Oceanography/Applied Ocean Science & Engineering,
Cambridge and Woods Hole, MA, USA*

²*Department of Mechanical Engineering, Massachusetts Institute of Technology,
Cambridge, MA*

(Dated: 17 February 2022)

1 The long baseline (LBL) underwater navigation paradigm relies on the conversion of
 2 recorded travel time to range to trilaterate for position. For real-time operations, this
 3 conversion assumes an isovelocity sound speed. For re-navigation in post-processing,
 4 computationally and/or labor intensive acoustic modeling may be employed to reduce
 5 uncertainty driven by multipath arrivals. This work demonstrates a real-time ray-
 6 based prediction method of the effective horizontal group speed to minimize vehicle
 7 position error. This method was implemented for a small scale AUV-LBL system in
 8 March 2020, in the Beaufort Sea, in total under-ice conditions and a double ducted
 9 acoustic propagation environment. The vehicle was successfully deployed and recov-
 10 ered. Given the lack of GPS data throughout the vehicle’s mission, however, the
 11 localization performance between GPS-linked beacon-to-beacon connections serves
 12 as a proxy for the effectiveness of this approach. The real-time positioning error
 13 between beacons was roughly 11 meters at distances up to 3 km, matching the mag-
 14 nitude of corrections recorded by the AUV during field operations. In post-processing,
 15 the localization performance is reevaluated with an operationally equivalent naviga-
 16 tion stack using modeled, historical, and locally observed sound speed profiles for
 17 a Minimal Bounce Criteria (MBC), as deployed in real-time, and an improved ray
 18 filtering algorithm, the Nearest Bounce Criteria (NBC). The best performing median
 19 re-positioning errors by bounce criterias are roughly 10 and 2 meters, respectively.
 20 Further investigation suggests that the GNSS ground truth data have some noise
 21 that is not reciprocated in the travel time data. Re-trilateration suggests that this
 22 approach effectively extends the single meter accuracy of the deployed GNSS pucks

into the water column.

^aebhatt@whoi.edu

^bhenrik@mit.edu

I. INTRODUCTION

Autonomous underwater vehicles (AUVs) are increasingly capable platforms to explore and sample the ocean, particularly for remote and/or dangerous regions. However, navigation uncertainty is a major challenge in considering AUVs as standard tools for oceanographic research. While land and air-based robots utilize information from Global Navigation Satellite Systems (GNSS) to achieve stunning location accuracy and precision throughout the duration of their missions, AUVs cannot access GNSS while underwater due to the rapid attenuation of electromagnetic waves. Therefore, underwater vehicles have relied on any combination of dead reckoning, hydrodynamic models, inertial navigation systems, doppler velocity logs, and acoustic baseline positioning systems for navigation (Paull *et al.*, 2014). Limiting navigation error and drift requires an AUV to periodically stall on the surface and obtain a GNSS fix to reset its position error. This foolproof method of self-positioning is undesirable for stealth, adverse weather conditions, and mission efficiency, and inaccessible in a GPS-denied situation like an ice-covered environment.

Of acoustic baseline navigation systems, long baseline (LBL) is the most GPS-like in style and scale, and most appropriate for mitigating drift without overburdening computation or payload size on the vehicle (Paull *et al.*, 2014; Van Uffelen, 2021). The state-of-the-art for LBL outsources depth to a pressure sensor and solves the two-dimensional localization problem by assuming an isovelocity, linear scaling between one way travel time (OWTT) and range (Eustice *et al.*, 2006, 2007; Webster *et al.*, 2009, 2012). This assumption is valid for short scale operations but oversimplifies propagation for larger and/or complex acoustic

environments. This paper demonstrates an embedded model-aided data processing approach to convert recorded OWTTs into pseudorange estimates. This approach was necessitated by total under-ice conditions and a double ducted acoustic environment, in the Beaufort Sea, in March 2020, for an AUV deployment during the Ice Exercise 2020 (ICEX20). We quantify the success of the proposed acoustic ranging method using GPS-linked beacon-to-beacon communication events, as the AUV-LBL positioning has no ground truth GNSS to compare to.

For clarity, we introduce definitions for timing, positioning, and navigation.

While RAFOS floats have championed one way ranging for re-positioning (Duda *et al.*, 2006; Rossby *et al.*, 1986), the ability to do so for navigation was facilitated by the advent of the WHOI micro-modem (Singh *et al.*, 2006) and synchronized chip scale atomic clocks (Gardner and Collins, 2016). Several short range (less than ten kilometers) navigation efforts have achieved minimal error with a nominal sound speed value (Eustice *et al.*, 2007; Kepper *et al.*, 2017; Webster *et al.*, 2009). However, these efforts were all conducted with X sound speed conditions. The approach in this paper, and other related works, was specifically designed to... the recently observed double ducted sound speed profile... For convenience, we call this phenomena the Beaufort Lens, with the lens referring to ...

There is no comparable work in the Arctic for a short scale AUV deployment in the Beaufort Lens. Both seminal and more recent AUV deployments witnessed the classical upward refracting sound speed profile that is amenable to an isovelocity simplification. Of note are large scale glider deployments; these, however, operated at X depths, X spatial scales, and did not need precise navigation because they experienced little to no sea ice. At

larger scales on the order of hundreds of kilometers, a deterministic (Graupe *et al.*, 2019) or through-the-sensor (Webster *et al.*, 2015) value for sound speed was used, but error remained in the hundreds of meters. The sound speed value was chosen by...

The navigation approach proposed includes a non-deterministic relationship between travel time and range previously limited to large scale re-navigation and re-positioning efforts. Such post-processing efforts can utilize additional information or computation that is inaccessible for onboard computation.

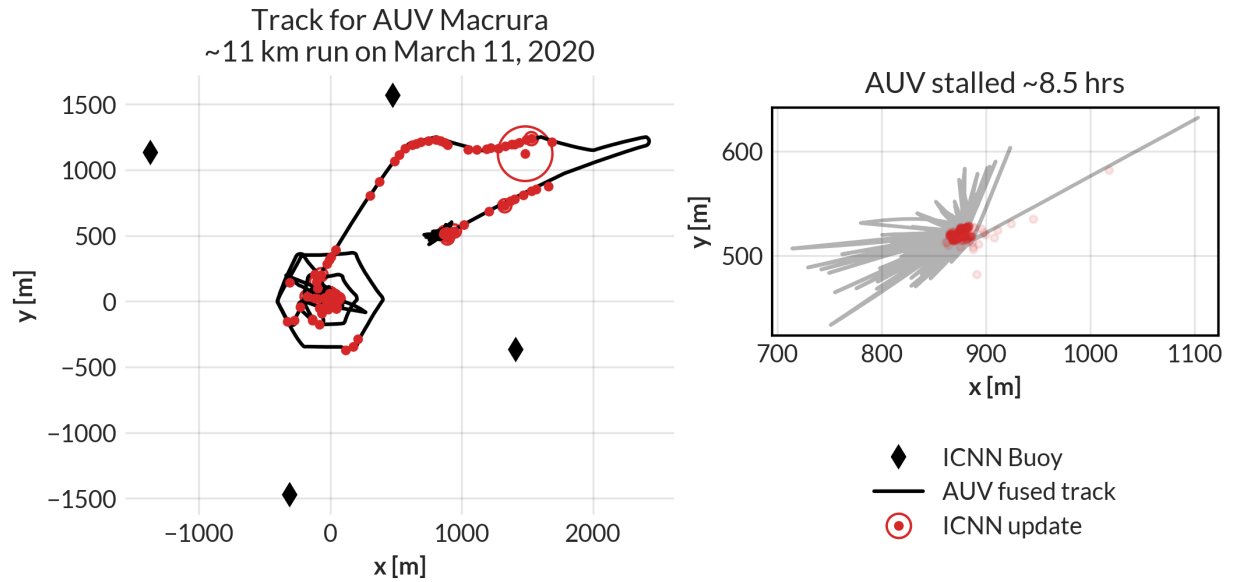


FIG. 1. The under-ice mission track for AUV Macrura, including the position updates as it stalled underneath the ice overnight. A marker was placed on the ice at the vehicle’s estimated self-location. It was recovered after a three day storm within a meter of the marker.

74 II. ICEX20 CONDITIONS AND EXPERIMENT DESIGN

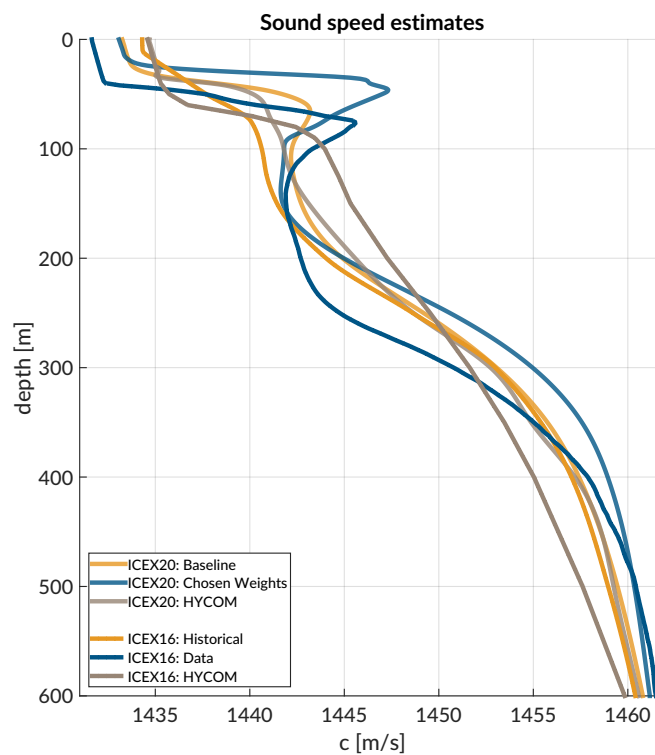


FIG. 2. Anticipated sound speed conditions: finish this using stuff from ICEX16, HYCOM, ITP

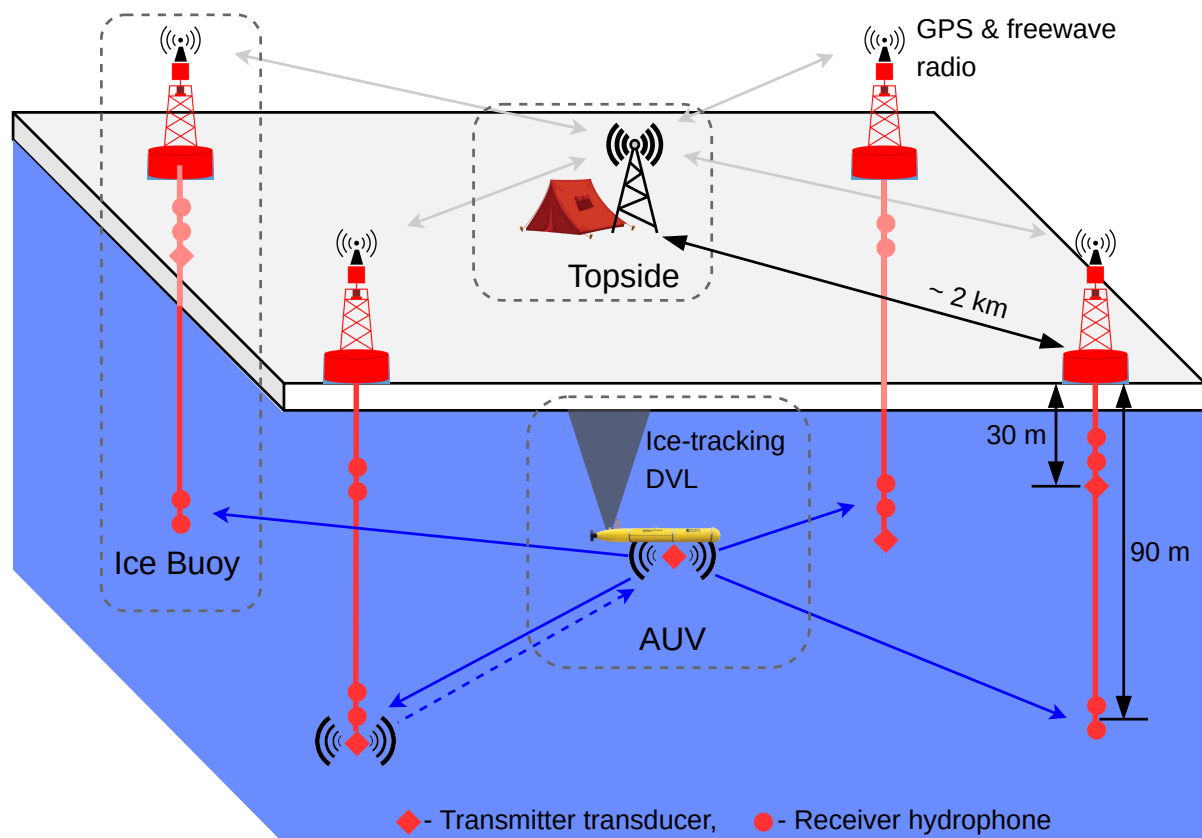


FIG. 3. A schematic overview of the Integrated Communication and Navigation Network (ICNN), which provides joint data-transfer and tracking between AUV and a human decision maker at Topside.

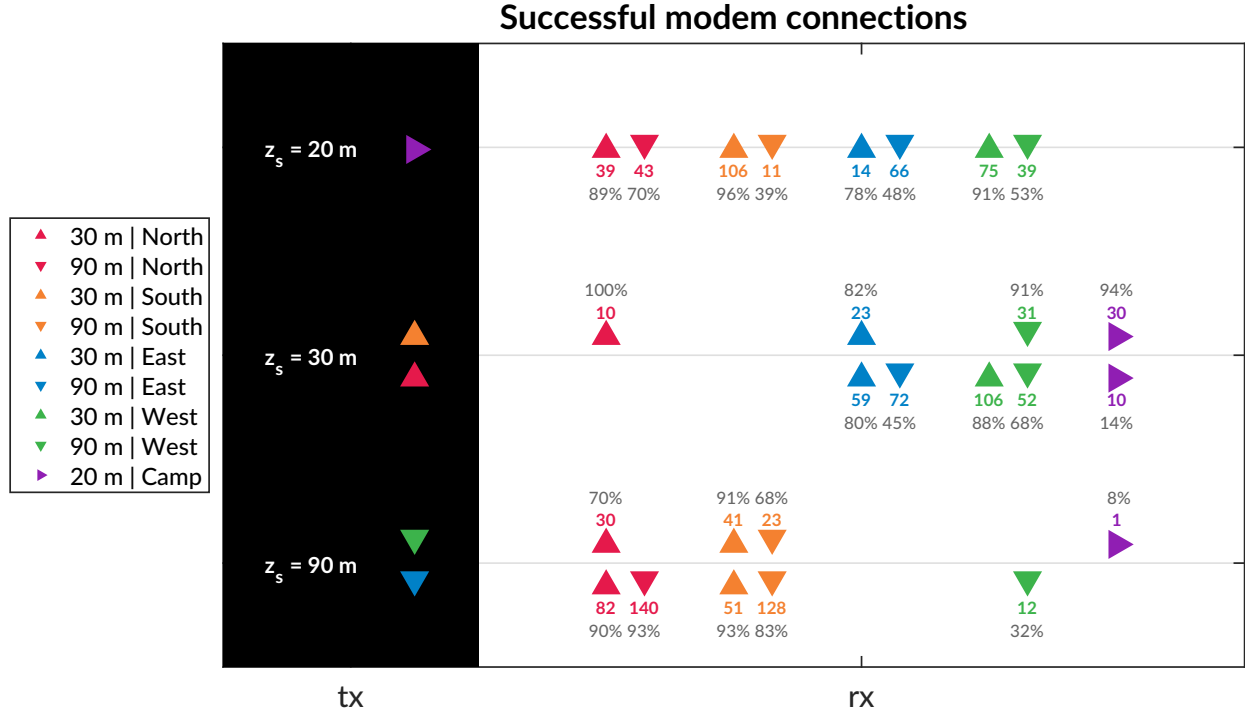


FIG. 4. An overview of the modem experiment by source and receiver depth and position. The black column on the left, tx , shows the source depth, z_s . The column on the right, rx , shows the receivers with the amount of good contacts. The orientation of the triangles—sideways, upwards, and downwards—corresponds to depths of 20, 30, and 90 m.

III. REAL-TIME PSEUDORANGE ANALYSIS

A. Minimal bounce criteria (MBC)

B. Pseudorange error metrics

C. Inherent overestimation from the minimal bounce criteria

1. Source depth of 20 m

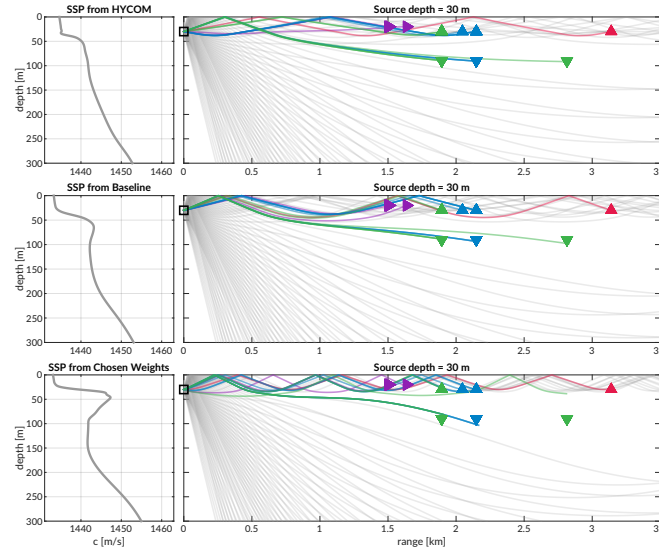


FIG. 5. Eigenrays for beacon to beacon events for each sound speed with a nominal source depth of 30 m. The beacons are highlighted in color/marker coding in Fig. 4. The eigenrays are curated from BELLHOP by travel time proximity and are traced in the representative receiver colors over a total ray fan in gray.

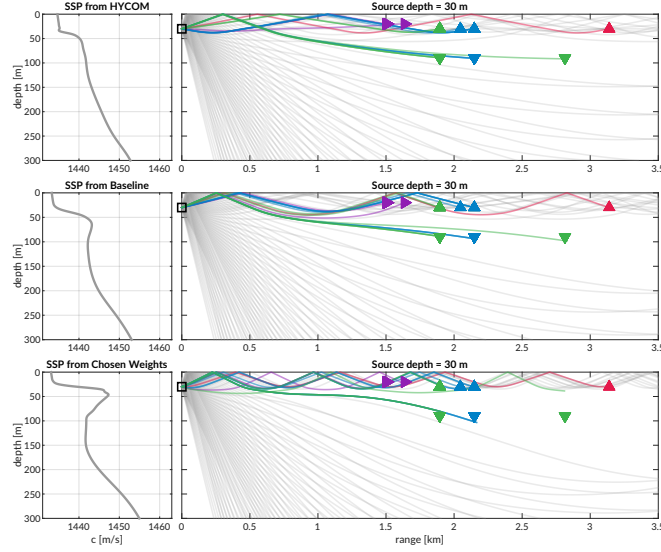


FIG. 6. Eigenrays for beacon to beacon events for each sound speed with a nominal source depth of 30 m. The beacons are highlighted in color/marker coding in Fig. 4. The eigenrays are curated from BELLHOP by travel time proximity and are traced in the representative receiver colors over a total ray fan in gray.

80 *2. Source depth of 30 m*

81 *3. Source depth of 90 m*

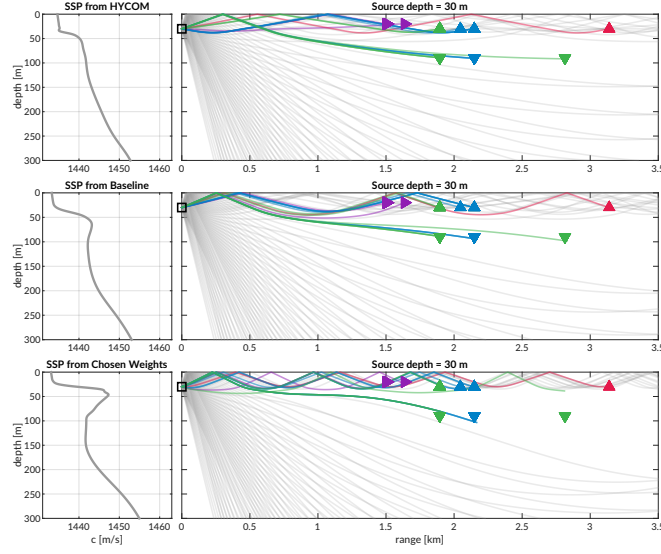


FIG. 7. Eigenrays for beacon to beacon events for each sound speed with a nominal source depth of 30 m. The beacons are highlighted in color/marker coding in Fig. 4. The eigenrays are curated from BELLHOP by travel time proximity and are traced in the representative receiver colors over a total ray fan in gray.

82 IV. POST-PROCESSED PSEUDORANGE ANALYSIS

83 A. Nearest bounce criteria (NBC)

84 B. Effective sound speed predictions

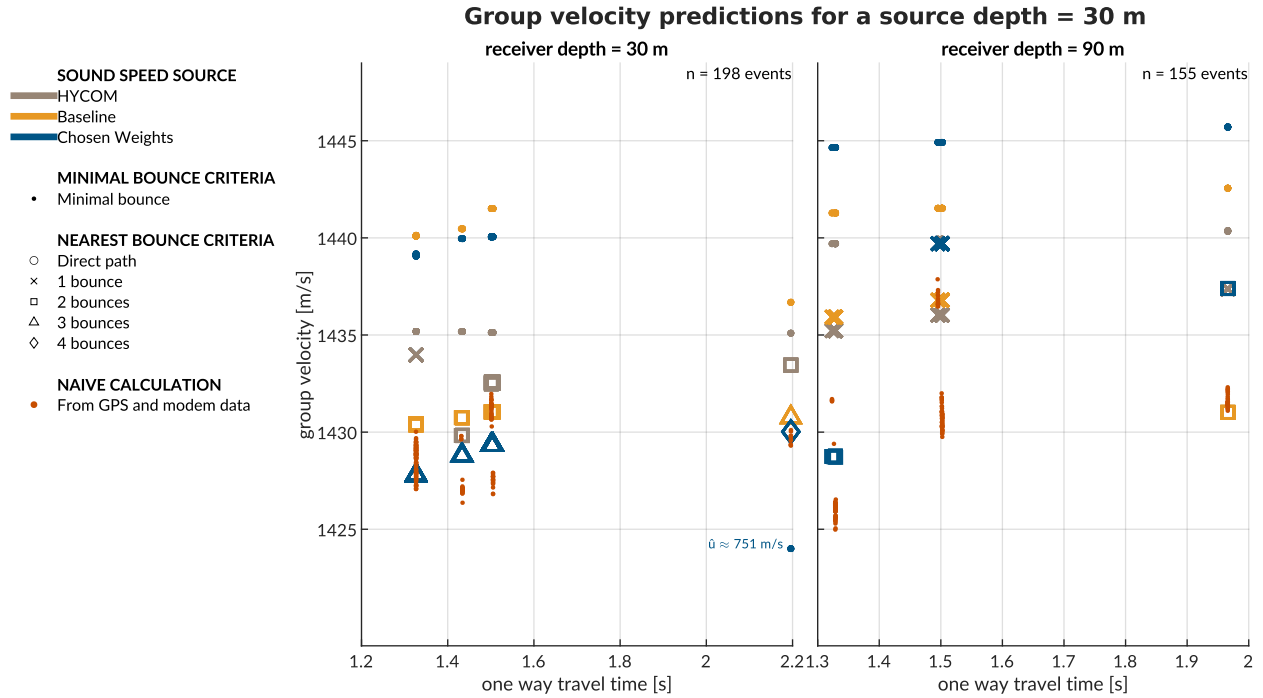


FIG. 8. A comparison of group velocity predictions for all beacon to beacon events in post-processing with a source depth of 30 m, with group velocity on the y-axis and recorded travel time on the x-axis. The left panel is for a receiver depth of 30 m; the right panel for 90 m. The sound speed source is indicated by color. The minimal and nearest bounce criterion are distinguished by different marker shapes, compared to the separately colored red dots showing the naive, data-driven group velocity calculation.

85

C. Pseudorange error metrics

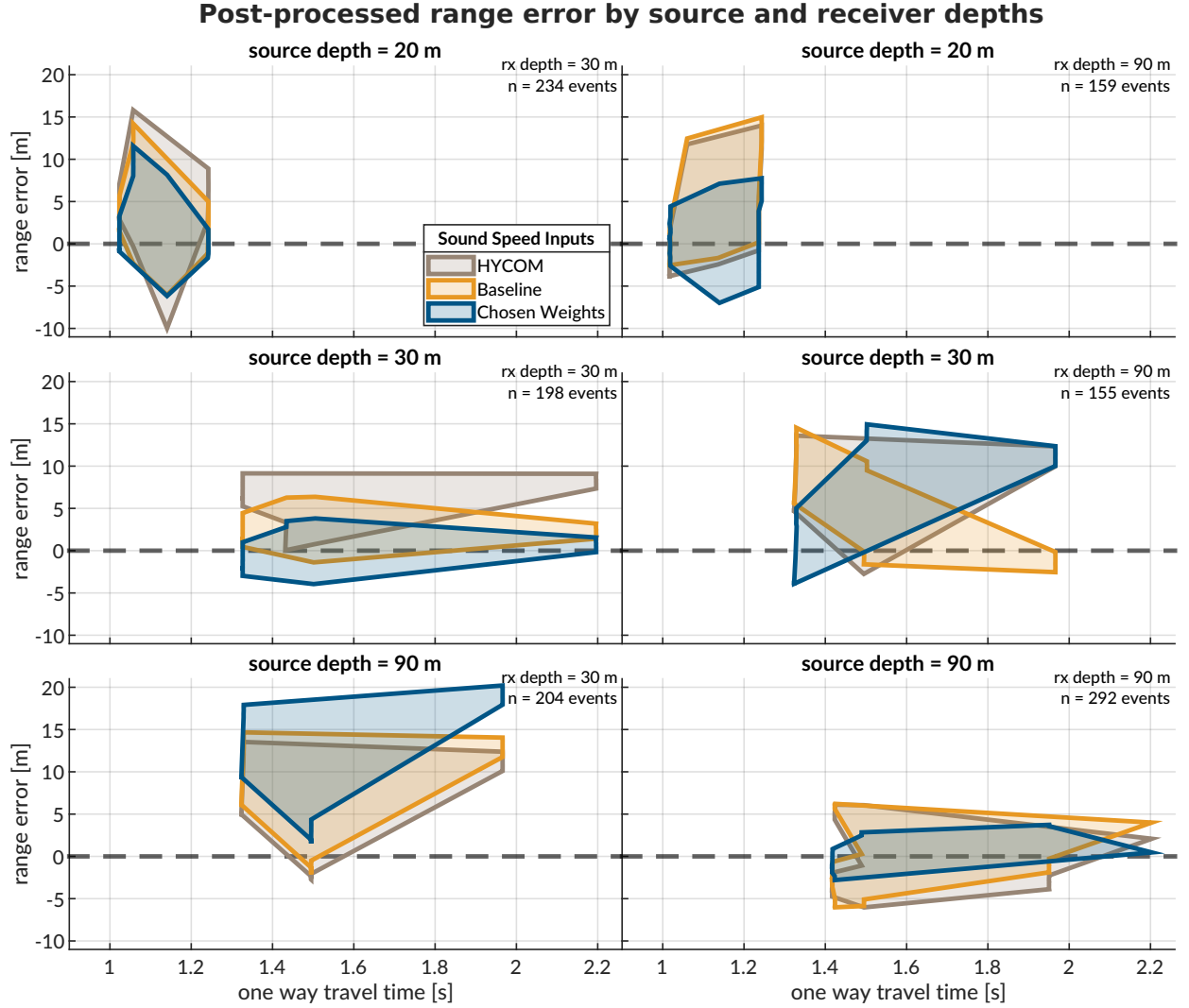


FIG. 9. The post-processed range error for source depths of 20, 30, and 90 m, and receiver depths of 30 and 90 m. The dashed gray line shows no error. The shaded region connects the range performance across all events.

86

V. RE-POSITIONING USING THE NEAREST BOUNCE CRITERIA

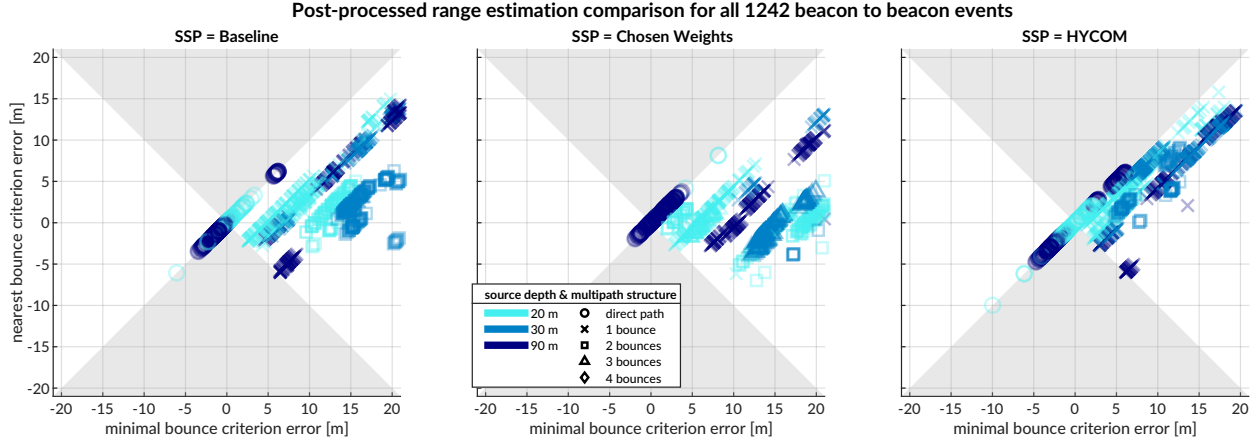


FIG. 10. A comparison of range estimation error for all beacon to beacon events in post-processing.

From left to right, the SSPs are the baseline, the chosen weights, and HYCOM. The colors indicate the source depth, darkening with depth, and the shapes indicate the multipath structure. Because this plot is square, the shaded region shows where the updated algorithm is less accurate than the *in situ* algorithm.

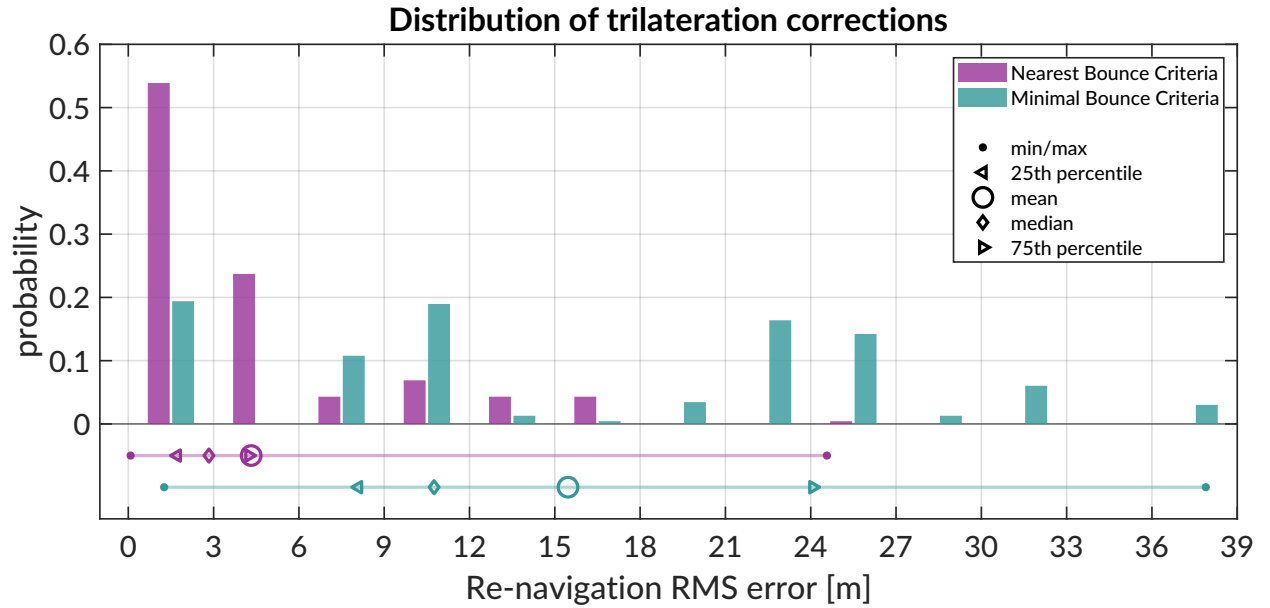


FIG. 11. WRITE THIS.

VI. RE-NAVIGATING AUV DATA

FIG A – error for MBC/NBC (Oscar Fig 6.17). Think about whether to include separate in situ column. Explain why this section uses error whereas previous section uses correction.

I think if we go down this route, we can take out the GNSS noise section entirely. The POMA paper would go over GNSS noise at high latitudes, crossmap, and look at individual drifts. I do not think the crossmap needs to stay in this publication; given small numerical value of the re-positioning trilateration, I think the same point is made (in a better way, actually).

95 **VII. INVESTIGATING POTENTIAL GNSS NOISE**

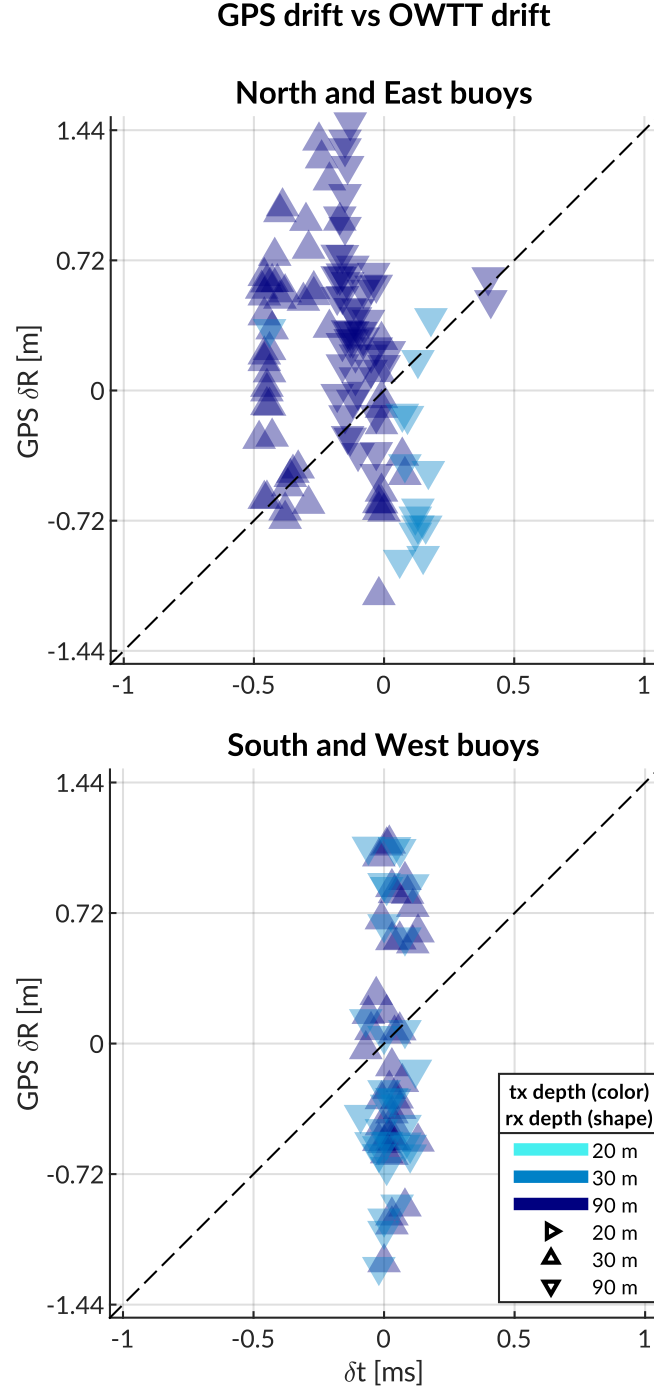


FIG. 12. A comparison of GPS drift (y-axis) versus OWTT drift (x-axis), colored by source and receiver depth. The physical link between North and East are shown on the top; South and West is on the bottom.

96 SUPPLEMENTARY FIGURES

97 Ice movement during the modem experiment

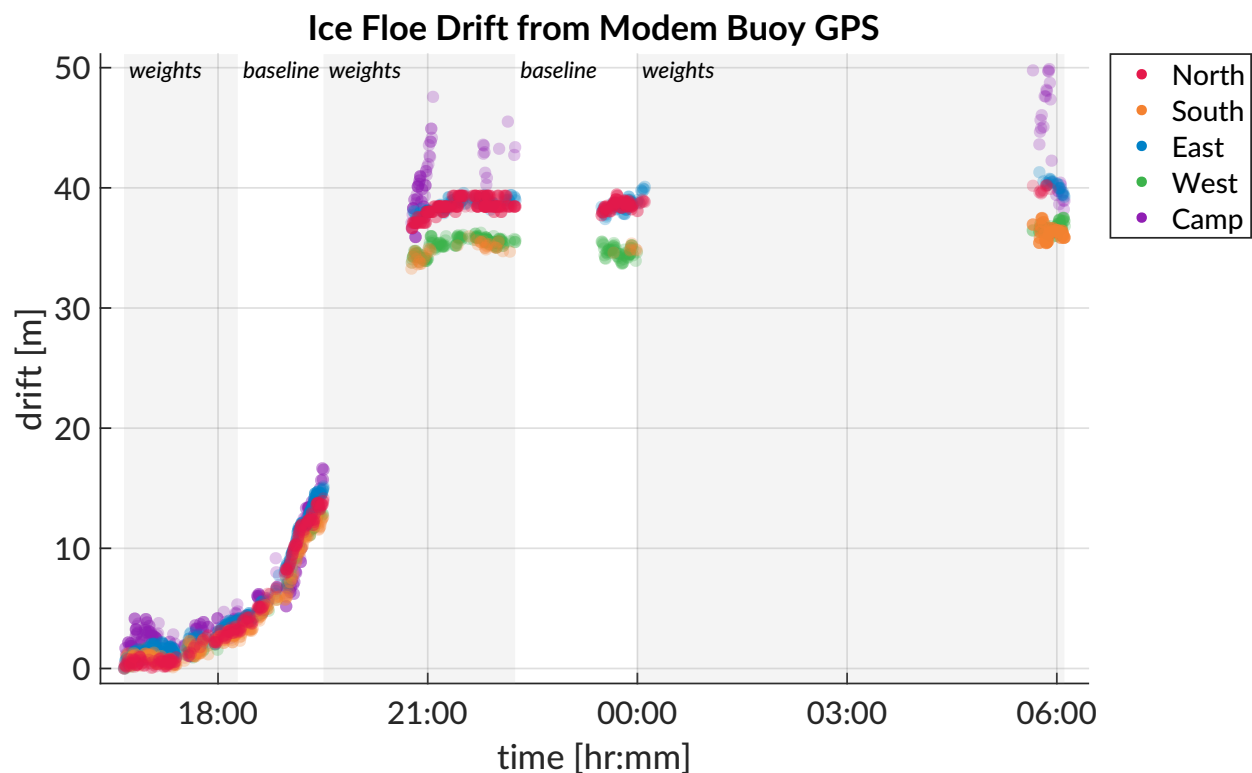


FIG. 13. The ICNN accounts for ice drift throughout the mission duration. This is the magnitude of the ice drift recorded, at each buoy, throughout the modem experiment. The shaded regions reference which sound speed estimate was used.

ACKNOWLEDGMENTS

We acknowledge the significant operational effort spearheaded by the LAMSS ICEX20 team and all our collaborators. Bhatt was funded by a National Defense, Science, and Engineering Graduate Fellowship. This work was supported by the Office of Naval Research 322-OA under ICEX20 (N00014-17-1-2474) and Task Force Ocean (N00014-19-1-2716).

- Duda, T. F., Morozov, A. K., Howe, B. M., Brown, M. G., Speer, K., Lazarevich, P., Worcester, P. F., and Cornuelle, B. D. (2006). “Evaluation of a Long-Range Joint Acoustic Navigation / Thermometry System,” pp. 1–6, doi: [10.1109/OCEANS.2006.306999](https://doi.org/10.1109/OCEANS.2006.306999).
- Eustice, R. M., Whitcomb, L. L., Singh, H., and Grund, M. (2006). “Recent Advances in Synchronous-Clock One-Way-Travel-Time Acoustic Navigation,” in *OCEANS 2006*, pp. 1–6, doi: [10.1109/OCEANS.2006.306931](https://doi.org/10.1109/OCEANS.2006.306931).
- Eustice, R. M., Whitcomb, L. L., Singh, H., and Grund, M. (2007). “Experimental Results in Synchronous-Clock One-Way-Travel-Time Acoustic Navigation for Autonomous Underwater Vehicles,” in *Proceedings 2007 IEEE International Conference on Robotics and Automation*, pp. 4257–4264, doi: [10.1109/ROBOT.2007.364134](https://doi.org/10.1109/ROBOT.2007.364134).
- Gardner, A., and Collins, J. (2016). “A second look at Chip Scale Atomic Clocks for long term precision timing,” OCEANS 2016 MTS/IEEE Monterey doi: [10.1109/OCEANS.2016.7761268](https://doi.org/10.1109/OCEANS.2016.7761268).

- Graupe, C. E., van Uffelen, L. J., Webster, S. E., Worcester, P. F., and Dzieciuch, M. A. (2019). “Preliminary results for glider localization in the Beaufort Duct using broadband acoustic sources at long range,” in *Oceans 2019 MTS/IEEE Seattle*, pp. 1–6, doi: [10.23919/OCEANS40490.2019.8962637](https://doi.org/10.23919/OCEANS40490.2019.8962637).
- Kepper, J. H., Claus, B. C., and Kinsey, J. C. (2017). “MEMS IMU and One-Way-Travel-Time Navigation for Autonomous Underwater Vehicles,” in *Oceans 2017 - Aberdeen*, Aberdeen, UK.
- Paull, L., Saeedi, S., Seto, M., and Li, H. (2014). “AUV Navigation and Localization: A Review,” *IEEE Journal of Oceanic Engineering* **39**(1), 131–149, <http://ieeexplore.ieee.org/document/6678293/>, doi: [10.1109/JOE.2013.2278891](https://doi.org/10.1109/JOE.2013.2278891).
- Rossby, T., Dorson, D., and Fontaine, J. (1986). “The RAFOS System,” *Journal of Atmospheric and Oceanic Technology* **3**(4), 672–679, https://journals.ametsoc.org/view/journals/atot/3/4/1520-0426_1986_003_0672_trs_2_0_co_2.xml, doi: [10.1175/1520-0426\(1986\)003<0672:TRS>2.0.CO;2](https://doi.org/10.1175/1520-0426(1986)003<0672:TRS>2.0.CO;2).
- Singh, S., Grund, M., Bingham, B., Eustice, R., Singh, H., and Freitag, L. (2006). “Underwater Acoustic Navigation with the WHOI Micro-Modem,” in *OCEANS 2006*, IEEE, Boston, MA, USA, pp. 1–4, <http://ieeexplore.ieee.org/document/4099008/>, doi: [10.1109/OCEANS.2006.306853](https://doi.org/10.1109/OCEANS.2006.306853).
- Van Uffelen, L. J. V. (2021). “Global Positioning Systems: Over Land and Under Sea,” *Acoustics Today* **17**(1), 9.
- Webster, S. E., Eustice, R. M., Singh, H., and Whitcomb, L. L. (2009). “Preliminary deep water results in single-beacon one-way-travel-time acoustic navigation for underwater

vehicles,” 2009 IEEE/RSJ International Conference on Intelligent Robots and Systems,
IROS 2009 2053–2060, doi: [10.1109/IROS.2009.5354457](https://doi.org/10.1109/IROS.2009.5354457).

Webster, S. E., Eustice, R. M., Singh, H., and Whitcomb, L. L. (2012). “Advances in
single-beacon one-way-travel-time acoustic navigation for underwater vehicles,” The In-
ternational Journal of Robotics Research **31**(8), 935–950, [https://doi.org/10.1177/](https://doi.org/10.1177/0278364912446166)
[0278364912446166](https://doi.org/10.1177/0278364912446166), doi: [10.1177/0278364912446166](https://doi.org/10.1177/0278364912446166).

Webster, S. E., Freitag, L. E., Lee, C. M., and Gobat, J. I. (2015). “Towards real-time under-
ice acoustic navigation at mesoscale ranges,” in *2015 IEEE International Conference on*
Robotics and Automation (ICRA), pp. 537–544, doi: [10.1109/ICRA.2015.7139231](https://doi.org/10.1109/ICRA.2015.7139231).